Letter

Search for the decay $B_s^0 \to \eta' K_S^0$

T. Pang,[74] V. Savinov,[74] I. Adachi,[21,17] H. Aihara,[90] D. M. Asner,[3] H. Atmacan,[8] V. Aulchenko,[4,70] T. Aushev,[23] R. Ayad,[84] V. Babu,[9] P. Behera,[29] K. Belous,[33] M. Bessner,[20] V. Bhardwaj,[26] B. Bhuyan,[27] T. Bilka,[5] A. Bobrov,[4,70] D. Bodrov,[23,48] G. Bonvicini,[94] J. Borah,[27] A. Bozek,[66] M. Bračko,[54,39] P. Branchini,[35] T. E. Browder,[20] A. Budano,[35] M. Campajola,[34,62] D. Červenkov,[5] P. Chang,[65] A. Chen,[64] B. G. Cheon,[19] K. Chilikin,[48] H. E. Cho,[19] K. Cho,[43] S.-J. Cho,[96] S.-K. Choi,[7] Y. Choi,[82] S. Choudhury,[37] D. Cinabro,[94] S. Cunliffe,[9] S. Das,[53] G. De Pietro,[35] R. Dhamija,[28] F. Di Capua,[34,62] J. Dingfelder,[2] Z. Doležal,[5] T. V. Dong,[11] D. Dossett,[56] S. Dubey,[20] D. Epifanov,[4,70] T. Ferber,[9] A. Frey,[16] B. G. Fulsom,[72] R. Garg,[73] V. Gaur,[93] N. Gabyshev,[4,70] A. Giri,[28] P. Goldenzweig,[40] E. Graziani,[35] T. Gu,[74] K. Gudkova,[4,70] C. Hadjivasiliou,[72] S. Halder,[85] K. Hayasaka,[68] H. Hayashii,[63] M. T. Hedges,[20] C.-L. Hsu,[83] T. Iijima,[61,60] K. Inami,[60] G. Inguglia,[32] A. Ishikawa,[21,17] R. Itoh,[21,17] M. Iwasaki,[71] Y. Iwasaki,[21] W. W. Jacobs,[30] E.-J. Jang,[18] S. Jia,[13] Y. Jin,[90] K. K. Joo,[6] J. Kahn,[40] D. Kalita,[27] A. B. Kaliyar,[85] K. H. Kang,[41] G. Karyan,[9] T. Kawasaki,[42] C. Kiesling,[55] C. H. Kim,[19] D. Y. Kim,[81] K.-H. Kim,[96] Y.-K. Kim,[96] K. Kinoshita,[8] P. Kodyš,[5] T. Konno,[42] A. Korobov,[4,70] S. Korpar,[54,39] E. Kovalenko,[4,70] P. Križan,[50,39] R. Kroeger,[57] P. Krokovny,[4,70] T. Kuhr,[51] R. Kumar,[75] K. Kumara,[94] A. Kuzmin,[4,70,48] Y.-J. Kwon,[96] Y.-T. Lai,[41] T. Lam,[93] J. S. Lange,[14] S. C. Lee,[46] C. H. Li,[49] J. Li,[46] L. K. Li,[8] Y. Li,[13] L. Li Gioi,[55] J. Libby,[29] K. Lieret,[51] D. Liventsev,[94,21] A. Martini,[97] M. Masuda,[89,76] T. Matsuda,[58] D. Matvienko,[4,70,48] F. Meier,[10] M. Merola,[34,62] F. Metzner,[40] K. Miyabayashi,[63] R. Mizuk,[48,23] G. B. Mohanty,[85] R. Mussa,[36] M. Nakao,[21,17] Z. Natkaniec,[66] A. Natochii,[20] L. Nayak,[28] M. Niiyama,[45] N. K. Nisar,[3] S. Nishida,[21,17] K. Ogawa,[68] S. Ogawa,[87] H. Ono,[67,68] P. Oskin,[48] P. Pakhlov,[48,59] G. Pakhlova,[23,48] S. Pardi,[34] H. Park,[46] S.-H. Park,[21] A. Passeri,[35] S. Patra,[26] S. Paul,[86,55] T. K. Pedlar,[52] R. Pestotnik,[39] L. E. Piilonen,[93] T. Podobnik,[50,39] V. Popov,[23] E. Prencipe,[24] M. T. Prim,[2] A. Rostomyan,[9] N. Rout,[29] G. Russo,[62] D. Sahoo,[37] S. Sandilya,[28] A. Sangal,[8] L. Santelj,[50,39] T. Sanuki,[88] G. Schnell,[1,25] Y. Seino,[68] K. Senyo,[95] M. E. Sevior,[56] M. Shapkin,[33] C. Sharma,[53] C. P. Shen,[13] J.-G. Shiu,[65] F. Simon,[55] J. B. Singh,[73,*] A. Sokolov,[33] E. Solovieva,[48] S. Stanič,[69] M. Starič,[39] J. F. Strube,[72] M. Sumihama,[15,76] T. Sumiyoshi,[92] M. Takizawa,[79,22,77] U. Tamponi,[36] K. Tanida,[38] N. Taniguchi,[21] F. Tenchini,[9] K. Trabelsi,[47] M. Uchida,[91] K. Uno,[68] S. Uno,[21,17] P. Urquijo,[56] R. Van Tonder,[2] G. Varner,[20] A. Vinokurova,[4,70] E. Waheed,[21] E. Wang,[74] M.-Z. Wang,[65] X. L. Wang,[13] M. Watanabe,[68] S. Watanuki,[96] E. Won,[44] X. Xu,[80] B. D. Yabsley,[83] W. Yan,[78] H. Ye,[9] J. Yelton,[12] J. H. Yin,[44] C. Z. Yuan,[31] Y. Zhai,[37] Z. P. Zhang,[78] V. Zhilich,[4,70] and V. Zhukova[48]

(Belle Collaboration)

[1]*Department of Physics, University of the Basque Country UPV/EHU, 48080 Bilbao*
[2]*University of Bonn, 53115 Bonn*
[3]*Brookhaven National Laboratory, Upton, New York 11973*
[4]*Budker Institute of Nuclear Physics SB RAS, Novosibirsk 630090*
[5]*Faculty of Mathematics and Physics, Charles University, 121 16 Prague*
[6]*Chonnam National University, Gwangju 61186*
[7]*Chung-Ang University, Seoul 06974*
[8]*University of Cincinnati, Cincinnati, Ohio 45221*
[9]*Deutsches Elektronen-Synchrotron, 22607 Hamburg*
[10]*Duke University, Durham, North Carolina 27708*
[11]*Institute of Theoretical and Applied Research (ITAR), Duy Tan University, Hanoi 100000*
[12]*University of Florida, Gainesville, Florida 32611*
[13]*Key Laboratory of Nuclear Physics and Ion-beam Application (MOE) and Institute of Modern Physics, Fudan University, Shanghai 200443*
[14]*Justus-Liebig-Universität Gießen, 35392 Gießen*
[15]*Gifu University, Gifu 501-1193*
[16]*II. Physikalisches Institut, Georg-August-Universität Göttingen, 37073 Göttingen*
[17]*SOKENDAI (The Graduate University for Advanced Studies), Hayama 240-0193*
[18]*Gyeongsang National University, Jinju 52828*
[19]*Department of Physics and Institute of Natural Sciences, Hanyang University, Seoul 04763*
[20]*University of Hawaii, Honolulu, Hawaii 96822*
[21]*High Energy Accelerator Research Organization (KEK), Tsukuba 305-0801*
[22]*J-PARC Branch, KEK Theory Center, High Energy Accelerator Research Organization (KEK), Tsukuba 305-0801*
[23]*National Research University Higher School of Economics, Moscow 101000*

[24]*Forschungszentrum Jülich, 52425 Jülich*
[25]*IKERBASQUE, Basque Foundation for Science, 48013 Bilbao*
[26]*Indian Institute of Science Education and Research Mohali, SAS Nagar, 140306*
[27]*Indian Institute of Technology Guwahati, Assam 781039*
[28]*Indian Institute of Technology Hyderabad, Telangana 502285*
[29]*Indian Institute of Technology Madras, Chennai 600036*
[30]*Indiana University, Bloomington, Indiana 47408*
[31]*Institute of High Energy Physics, Chinese Academy of Sciences, Beijing 100049*
[32]*Institute of High Energy Physics, Vienna 1050*
[33]*Institute for High Energy Physics, Protvino 142281*
[34]*INFN-Sezione di Napoli, I-80126 Napoli*
[35]*INFN-Sezione di Roma Tre, I-00146 Roma*
[36]*INFN-Sezione di Torino, I-10125 Torino*
[37]*Iowa State University, Ames, Iowa 50011*
[38]*Advanced Science Research Center, Japan Atomic Energy Agency, Naka 319-1195*
[39]*J. Stefan Institute, 1000 Ljubljana*
[40]*Institut für Experimentelle Teilchenphysik, Karlsruher Institut für Technologie, 76131 Karlsruhe*
[41]*Kavli Institute for the Physics and Mathematics of the Universe (WPI), University of Tokyo, Kashiwa 277-8583*
[42]*Kitasato University, Sagamihara 252-0373*
[43]*Korea Institute of Science and Technology Information, Daejeon 34141*
[44]*Korea University, Seoul 02841*
[45]*Kyoto Sangyo University, Kyoto 603-8555*
[46]*Kyungpook National University, Daegu 41566*
[47]*Université Paris-Saclay, CNRS/IN2P3, IJCLab, 91405 Orsay*
[48]*P.N. Lebedev Physical Institute of the Russian Academy of Sciences, Moscow 119991*
[49]*Liaoning Normal University, Dalian 116029*
[50]*Faculty of Mathematics and Physics, University of Ljubljana, 1000 Ljubljana*
[51]*Ludwig Maximilians University, 80539 Munich*
[52]*Luther College, Decorah, Iowa 52101*
[53]*Malaviya National Institute of Technology Jaipur, Jaipur 302017*
[54]*Faculty of Chemistry and Chemical Engineering, University of Maribor, 2000 Maribor*
[55]*Max-Planck-Institut für Physik, 80805 München*
[56]*School of Physics, University of Melbourne, Victoria 3010*
[57]*University of Mississippi, University, Mississippi 38677*
[58]*University of Miyazaki, Miyazaki 889-2192*
[59]*Moscow Physical Engineering Institute, Moscow 115409*
[60]*Graduate School of Science, Nagoya University, Nagoya 464-8602*
[61]*Kobayashi-Maskawa Institute, Nagoya University, Nagoya 464-8602*
[62]*Università di Napoli Federico II, I-80126 Napoli*
[63]*Nara Women's University, Nara 630-8506*
[64]*National Central University, Chung-li 32054*
[65]*Department of Physics, National Taiwan University, Taipei 10617*
[66]*H. Niewodniczanski Institute of Nuclear Physics, Krakow 31-342*
[67]*Nippon Dental University, Niigata 951-8580*
[68]*Niigata University, Niigata 950-2181*
[69]*University of Nova Gorica, 5000 Nova Gorica*
[70]*Novosibirsk State University, Novosibirsk 630090*
[71]*Osaka City University, Osaka 558-8585*
[72]*Pacific Northwest National Laboratory, Richland, Washington 99352*
[73]*Panjab University, Chandigarh 160014*
[74]*University of Pittsburgh, Pittsburgh, Pennsylvania 15260*
[75]*Punjab Agricultural University, Ludhiana 141004*
[76]*Research Center for Nuclear Physics, Osaka University, Osaka 567-0047*
[77]*Meson Science Laboratory, Cluster for Pioneering Research, RIKEN, Saitama 351-0198*
[78]*Department of Modern Physics and State Key Laboratory of Particle Detection and Electronics, University of Science and Technology of China, Hefei 230026*
[79]*Showa Pharmaceutical University, Tokyo 194-8543*
[80]*Soochow University, Suzhou 215006*
[81]*Soongsil University, Seoul 06978*

[82]*Sungkyunkwan University, Suwon 16419*
[83]*School of Physics, University of Sydney, New South Wales 2006*
[84]*Department of Physics, Faculty of Science, University of Tabuk, Tabuk 71451*
[85]*Tata Institute of Fundamental Research, Mumbai 400005*
[86]*Department of Physics, Technische Universität München, 85748 Garching*
[87]*Toho University, Funabashi 274-8510*
[88]*Department of Physics, Tohoku University, Sendai 980-8578*
[89]*Earthquake Research Institute, University of Tokyo, Tokyo 113-0032*
[90]*Department of Physics, University of Tokyo, Tokyo 113-0033*
[91]*Tokyo Institute of Technology, Tokyo 152-8550*
[92]*Tokyo Metropolitan University, Tokyo 192-0397*
[93]*Virginia Polytechnic Institute and State University, Blacksburg, Virginia 24061*
[94]*Wayne State University, Detroit, Michigan 48202*
[95]*Yamagata University, Yamagata 990-8560*
[96]*Yonsei University, Seoul 03722*
[97]*Deutsches Elektronen-Synchrotron, 22607 Hamburg*

(Received 5 January 2022; accepted 13 September 2022; published 22 September 2022)

We report the results of the first search for the decay $B_s^0 \to \eta' K_S^0$ using 121.4 fb^{-1} of data collected at the $\Upsilon(5S)$ resonance with the Belle detector at the KEKB asymmetric-energy e^+e^- collider. We observe no signal and set a 90% confidence-level upper limit of 8.16×10^{-6} on the $B_s^0 \to \eta' K_S^0$ branching fraction.

DOI: 10.1103/PhysRevD.106.L051103

The measurements of rare decays of hadrons containing the heavy b quark provide an indirect way to search for new hypothetical particles (see, e.g., Sec. 17.4 in [1]) and, generally, effects not described by the Standard Model (SM). In this paper we describe the first search for the decay $B_s^0 \to \eta' K_S^0$, a charmless decay with contributions from gluonic and electroweak penguin amplitudes. On the one hand, processes that include such amplitudes are sensitive to beyond-the-SM physics, which could affect decay rates and CP asymmetries [2]. On the other hand, even the SM-based theoretical predictions [3–7] for the decay $B_s^0 \to \eta' K_S^0$ vary between 0.72×10^{-6} and 4.5×10^{-6}, which makes measuring the branching fraction for the studied decay valuable in its own right.

The two-body decay searched for in the analysis described in this paper is also interesting because it includes η', the particle whose anomalous production in inclusive and exclusive B decays, first observed by the CLEO experiment more than two decades ago [8,9], became the catalyst for a large body of dedicated theoretical work [10], followed by a recent experimental study of $B_s^0 \to \eta' X_{s\bar{s}}$ at Belle using a semi-inclusive method [11]. While the large rate for exclusive decays, such as $B^\pm \to \eta' K^\pm$, could be accounted for by SM factorization [12], any process involving η', such as the decays of B_s^0 mesons, could provide valuable information about the role of this particle in decays of heavy flavors and has been an important part of motivation for the work presented here.

The search for the decay $B_s^0 \to \eta' K_S^0$ described in this paper is based on a data sample of 121.4 fb^{-1} collected with the Belle detector at the KEKB asymmetric-energy e^+e^- collider [13] when it operated at the $\Upsilon(5S)$ resonance. The Belle detector is a large-solid-angle magnetic spectrometer that consists of a silicon vertex detector, a 50-layer central drift chamber, an array of aerogel threshold Cherenkov counters, a barrel-like arrangement of time-of-flight scintillation counters, and a CsI(Tl) crystal-based electromagnetic calorimeter (ECL) located inside a superconducting solenoid coil that provided a 1.5 T magnetic field. An iron flux-return located outside of the coil is instrumented to detect K_L^0 mesons and to identify muons. The detailed description of the Belle detector could be found elsewhere [14].

There are three two-body decays of $\Upsilon(5S)$ that serve as sources of B_s^0 mesons: $B_s^{*0}\bar{B}_s^{*0}$, $B_s^{*0}\bar{B}_s^0$, or $B_s^0\bar{B}_s^{*0}$, and $B_s^0\bar{B}_s^0$. The first two channels have relative fractions of $f_{B_s^{*0}\bar{B}_s^{*0}} = (87.0 \pm 1.7)\%$ and $f_{B_s^0\bar{B}_s^{*0}} = (7.3 \pm 1.4)\%$ [15]. We reconstruct signal B_s^0 mesons coming directly from $\Upsilon(5S)$ decay or from the radiative decay of the excited vector state B_s^{*0} (the charge-conjugate decay mode is included throughout this paper). The $\Upsilon(5S)$ resonance production cross section is 340 ± 16 pb [15], and f_s, its total branching fraction for decays to $B_s^{(*)0}\bar{B}_s^{(*)0}$, is 0.201 ± 0.031 [16]. Therefore, the Belle data sample is estimated to

[*]University of Petroleum and Energy Studies, Dehradun 248007.

contain $(16.60 \pm 2.68) \times 10^6$ B_s^0 mesons. We obtain the results for the branching fraction $\mathcal{B}(B_s^0 \to \eta' K_S^0)$ as well as for the product $f_s \times \mathcal{B}(B_s^0 \to \eta' K_S^0)$.

We use Monte Carlo (MC) generator EVTGEN [17] to simulate the production and decay processes, and GEANT toolkit [18] to model detector response. To validate our analysis methods and to calibrate parameters of signal probability density function (PDF), we use a control sample of two-body decays $B^0 \to \eta' K_S^0$ reconstructed in 711 fb^{-1} of $\Upsilon(4S)$ data collected by Belle at $\Upsilon(4S)$.

To search for $B_s^0 \to \eta' K_S^0$ decay, we first reconstruct $K_S^0 \to \pi^+\pi^-$ and $\eta' \to \eta\pi^+\pi^-$ followed by the decay $\eta \to \gamma\gamma$. For charged pions from η' decay we require the distance of closest approach to the interaction point to be less than 4 cm along the z axis and less than 0.3 cm in the direction perpendicular to it, where the z axis is opposite to the direction of the e^+ beam. Transverse momenta of these charged pion candidates are required to exceed 100 MeV/ c. To distinguish between charged pions and other particles, we apply requirements on the likelihood ratio, $R_{h/\pi} = L_\pi/(L_\pi + L_h)$, which is based on particle identification (PID, see Chap. 5 in [1]) measurements, where L_π is the likelihood for the track according to pion hypothesis, and L_h is for kaon ($h = K$) or electron ($h = e$) hypotheses. By requiring $R_{K/\pi} \leq 0.6$ and $R_{e/\pi} \leq 0.95$ for charged pion candidates we reject 25.8% of background events while the signal efficiency loss is 7.6%. Photons are reconstructed as ECL energy clusters not matched to any charged tracks. We require the reconstructed laboratory-frame energy of photon candidates in the barrel (endcap) region of ECL to exceed 50 (100) MeV. Barrel region of ECL covers polar angle θ between 32.2° and 128.7°, where the angle θ is measured with respect to the z axis in the laboratory frame. θ coverage of forward and backward endcaps is between 12.0° and 31.4°, and 131.5° and 157.2°, respectively. The η candidates are reconstructed using the decay channel $\eta \to \gamma\gamma$, with the reconstructed invariant mass of each candidate required to be between 0.515 GeV$/c^2$ and 0.580 GeV$/c^2$, which corresponds, approximately, to a $\pm 3\sigma$ Gaussian resolution window around the nominal η mass [16]. To suppress combinatorial background arising due to low-energy photons, the magnitude of the cosine of the helicity angle ($\cos\theta_{\rm hel}$) is required to be less than 0.97, where $\theta_{\rm hel}$ is the angle in the rest frame of the η candidate between the directions of its Lorentz boost from the laboratory frame and one of the photons. This requirement rejects 11.4% of background events while the efficiency loss for signal events is 3.0%. We perform kinematic fits constraining the reconstructed masses of the η candidates to the nominal η mass [16]. Then η' candidates are reconstructed using η candidates and pairs of oppositely charged tracks identified as pions within a wide window of the reconstructed invariant mass $M(\pi^+\pi^-\eta)$ between 0.920 GeV$/c^2$ and 0.980 GeV$/c^2$, which corresponds, approximately, to the range $[-10, +6]\sigma$ of the Gaussian resolution and includes a wide sideband, so $M(\pi^+\pi^-\eta)$ could be used to extract the signal, as described later in this paper. To identify the K_S^0 candidates, we use a neural network technique [19] to search for secondary vertices associated with pairs of oppositely charged tracks treated as pions [20]. To improve mass resolution, a kinematic fit is performed to the vertex. To reconstruct a B_s^0 candidate, we combine K_S^0 and η' candidates after constraining the reconstructed mass of the η' to the nominal η' mass [16]. We further select B_s^0 candidates using three kinematic variables: beam-energy-constrained B_s^0 mass $M_{\rm bc} = \sqrt{E_{\rm beam}^2 - p_{B_s^0}^2}$, the energy difference $\Delta E = E_{B_s^0} - E_{\rm beam}$, and $M(\pi^+\pi^-\eta)$, where $E_{\rm beam}$ is the beam energy, and $E_{B_s^0}$ and $p_{B_s^0}$ are the reconstructed energy and momentum of the B_s^0 candidate, respectively, calculated in the e^+e^- center-of-mass frame. Signal B_s^0 candidates are required to satisfy 5.300 GeV$/c^2 < M_{\rm bc} <$ 5.440 GeV$/c^2$ and -0.400 GeV $< \Delta E <$ 0.300 GeV.

The main source of background to our signal is hadronic continuum, i.e., quark-pair production in e^+e^- annihilation. To suppress continuum background, we take advantage of the difference between signal and background event topologies by utilizing a set of 17 modified Fox-Wolfram moments [21]. By optimizing Fisher discriminant [22] coefficients evaluated using these moments, we calculate a likelihood ratio ($\mathcal{R}_{s/b}$) according to signal and background hypotheses. To suppress background, we require $\mathcal{R}_{s/b} > 0.6$. This 80.5%-efficient requirement removes 90.0% of continuum background. The details of our continuum suppression algorithm are provided elsewhere [23].

After applying the described selection criteria, 16% of signal MC events have more than one candidate. We select the best candidate with the smallest value of $\chi^2 = \chi^2_\eta + \chi^2_{\pi^+\pi^-} + \chi^2_{\eta':\pi^+\pi^-}$, where $\chi^2_\eta = (\frac{M_{\gamma\gamma} - m_\eta}{\sigma_{\gamma\gamma}})^2$ is from the kinematic fit for the η candidate, $\chi^2_{\pi^+\pi^-}$ is from the vertex fit for pion candidates from the K_S^0 decay, and $\chi_{\eta':\pi^+\pi^-}$ is from fitting charged pion tracks from η' decay to a common vertex. This method chooses the correct B_s^0 candidate 91% of the time in signal MC events. The overall reconstruction efficiency in this analysis is 26.8%.

To extract the signal yield, we perform a three-dimensional (3D) unbinned extended maximum likelihood (ML) fit to $M_{\rm bc}$, ΔE, and $M(\pi^+\pi^-\eta)$. The likelihood function is defined as

$$\mathcal{L} = \frac{e^{-\sum_j^{b,s} N_j}}{N!} \prod_{i=1}^{N} \left(\sum_j^{b,s} N_j \mathcal{P}_j [M_{\rm bc}^i, \Delta E^i, M^i(\pi^+\pi^-\eta)] \right), \quad (1)$$

where N is the total number of events in the sample, N_j are the fit parameters for the number of signal ($j = s$) and background events ($j = b$), $\mathcal{P}_j$ are the PDFs for the signal and background components of our fitting model.

The background PDF is further represented by the sum of two 3D PDFs which describe a peaking $M^i(\pi^+\pi^-\eta)$ component with real η' mesons and a nonpeaking component of combinatorial origin. Since the correlations among these three fitting variables are small, each of the three 3D PDFs describing the signal contribution, and the peaking and nonpeaking backgrounds, is assumed to factorize as

$$\mathcal{P}_j[M_{\rm bc}, \Delta E, M(\pi^+\pi^-\eta)] = \mathcal{P}_j[M_{\rm bc}] \times \mathcal{P}_j[\Delta E] \times \mathcal{P}_j[M(\pi^+\pi^-\eta)]. \qquad (2)$$

The signal component is further described by the sum of contributions from three signal sources $B_s^{*0}\bar{B}_s^{*0}$, $B_s^{*0}\bar{B}_s^0$ or $B_s^0\bar{B}_s^{*0}$, and $B_s^0\bar{B}_s^0$, with relative fractions for the two former contributions according to their branching fractions [15].

The signal $M_{\rm bc}$ distribution is modeled with a Gaussian, and that of ΔE by the sum of a Gaussian and Crystal Ball function [24] (with different means). A sum of two Gaussians with the same mean is used to describe the reconstructed invariant mass of η' candidates in signal events.

To model the background $M_{\rm bc}$ distribution, an ARGUS [25] function with a fixed endpoint at 5.433 GeV$/c^2$ is used. We use a second-order Chebyshev polynomial to describe the background ΔE distribution. To account for the presence of real η' mesons in background events, we use the signal $M(\pi^+\pi^-\eta)$ PDF to model the peaking part and a first-order Chebyshev polynomial to model the nonpeaking component.

To obtain PDF shape parameters for signal, we first use the $\Upsilon(5S)$ signal MC sample and determine the peak positions for $M_{\rm bc}$ and ΔE. Then we use $\Upsilon(4S)$ data for the decay $B^0 \to \eta' K_S^0$ to determine all the other PDF parameters. To obtain background PDF shapes, we use $\Upsilon(5S)$ sideband data collected outside of the signal region defined as $5.401\ \text{GeV}/c^2 < M_{\rm bc} < 5.423\ \text{GeV}/c^2$ and $-0.200\ \text{GeV} < \Delta E < 0.100\ \text{GeV}$, and $0.940\ \text{GeV}/c^2 < M(\pi^+\pi^-\eta) < 0.970\ \text{GeV}/c^2$.

To validate our $\Upsilon(5S)$ analysis, we use the full Belle data sample collected at $\Upsilon(4S)$ energy to analyze the decay $B^0 \to \eta' K_S^0$. The results of the fit to $\Upsilon(4S)$ data are shown in Fig. 1, where each fit projection is plotted after additional selection criteria are applied to the other two variables, $0.948\ \text{GeV}/c^2 < M(\pi^+\pi^-\eta) < 0.966\ \text{GeV}/c^2$, $5.274\ \text{GeV}/c^2 < M_{\rm bc} < 5.286\ \text{GeV}/c^2$, and $-0.100\ \text{GeV} < \Delta E < 0.060\ \text{GeV}$. We estimate the branching fraction, $\mathcal{B}(B^0 \to \eta' K^0) = (52.3 \pm 2.1) \times 10^{-6}$ (where only the statistical uncertainty is shown), which is consistent with our previous result [26] within the estimated systematic uncertainties.

To extract the signal yield at $\Upsilon(5S)$, we fix all PDF shape parameters to the values obtained from our MC-assisted data-based studies, except for the fraction of background containing real η' mesons, which remains a free parameter in our final fit. To obtain our nominal result, we fit the data with the following three floating parameters in the fit: the number of signal events N_s, the number of background events N_b, and the fraction of background with real η' mesons.

By performing a 3D fit to $\Upsilon(5S)$ data, we obtain -3.21 ± 1.85 signal and 801 ± 28 background events. The results of the fit are plotted in Fig. 2. To emphasize the dominant signal source, $B_s^{*0}\bar{B}_s^{*0}$, each fit projection in this figure is plotted after additional selection criteria are applied to the other two variables, $0.948\ \text{GeV}/c^2 < M(\pi^+\pi^-\eta) < 0.966\ \text{GeV}/c^2$, $5.400\ \text{GeV}/c^2 < M_{\rm bc} < 5.440\ \text{GeV}/c^2$, and $-0.100\ \text{GeV} < \Delta E < 0.060\ \text{GeV}$. We observe no signal and estimate the upper limits for the branching fraction and its product with f_s.

Sources of systematic uncertainties and their contributions are summarized in Table I. The relative uncertainties for f_s and $\sigma(\Upsilon(5S))$ are 15.4% [16] and 4.7% [15], respectively. Systematic uncertainty due to $f_{B_s^{(*)0}\bar{B}_s^{(*)0}}$, i.e., relative contributions of the three signal sources, is 1.87%, estimated by varying the relative fractions of the three contributions to signal PDF. For daughter branching

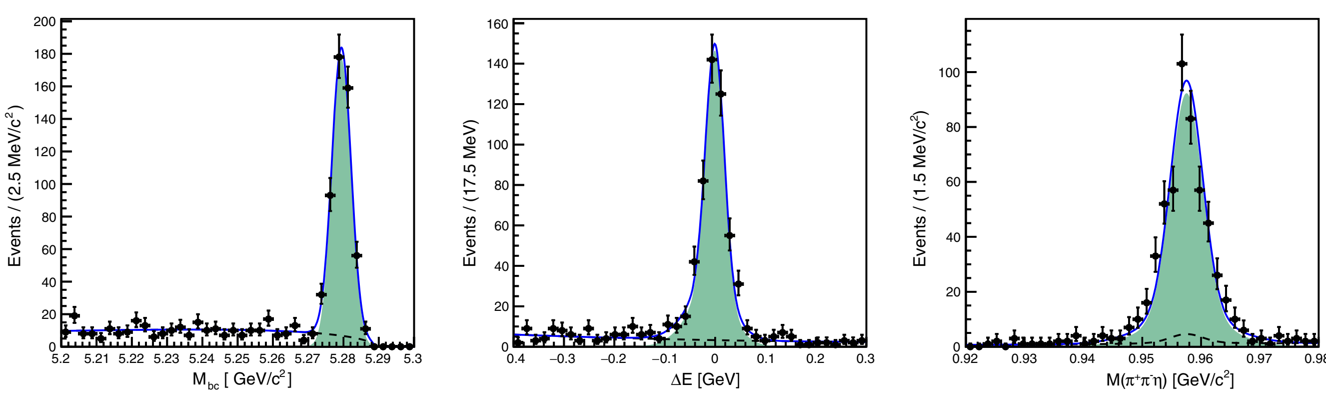

FIG. 1. Signal region fit projections onto $M_{\rm bc}$, ΔE and $M(\pi^+\pi^-\eta)$ for $B^0 \to \eta' K_S^0$ event candidates in $\Upsilon(4S)$ data after additional selection criteria are applied, as described in the text. Points with the error bars show the binned data. Blue solid lines show the results of the fit, filled area and black dashed line show the signal and background fit components, respectively.

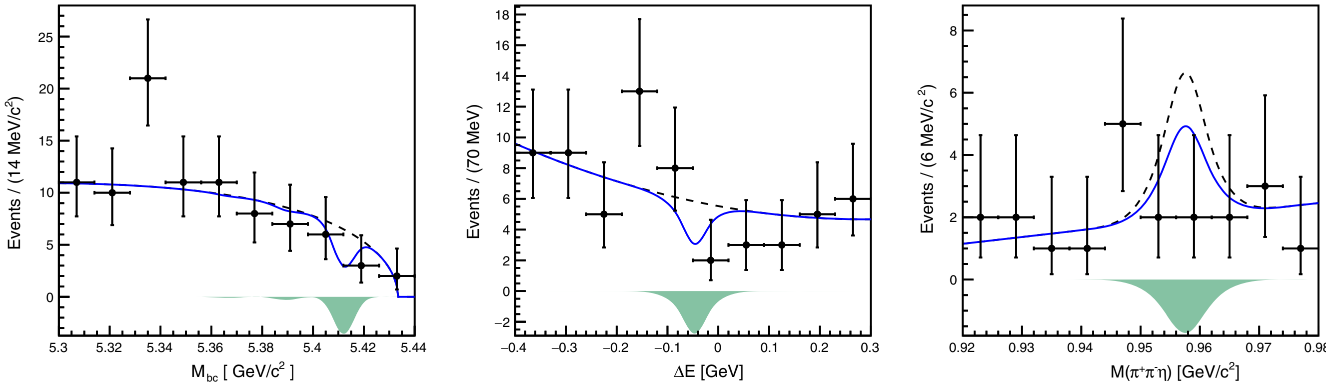

FIG. 2. Signal region fit projections onto $M_{\rm bc}$, ΔE and $M(\pi^+\pi^-\eta)$ for $B_s^0 \to \eta' K_S^0$ event candidates in $\Upsilon(5S)$ data after additional selection criteria are applied, as described in the text. Points with the error bars show the binned data. Blue solid lines show the results of the fit, filled area and black dashed line show the signal and background fit components, respectively.

fractions, the uncertainties for $\eta \to \gamma\gamma$, $\eta' \to \eta\pi^+\pi^-$, and $K_S^0 \to \pi^+\pi^-$ are 0.2%, 0.7%, and 0.05%, respectively [16]. Statistical uncertainty due to MC statistics is 0.11% via $\sqrt{\epsilon \times (1-\epsilon)/N}$, where N is the total number of signal MC events, and ϵ is the overall reconstruction efficiency. The uncertainties in π, η, and K_S^0 reconstruction efficiencies are 1.4% (0.35% per track [27]), 4.1% [28], and 1.4% [29] per particle, respectively. The uncertainty due to PDF parametrization is 11.9%, estimated from the change in signal yield while varying fixed PDF shape parameters one at a time by one unit of their Gaussian uncertainties as measured from the control data sample for signal and from data sideband for background.

The uncertainty from PID selection is 2.4% [27]. By comparing the $\mathcal{R}_{s/b}$ distributions for $B_s^0 \to K_S^0\eta'$ events in $\Upsilon(4S)$ data and signal MC events, we estimate the uncertainty in the efficiency of likelihood ratio requirement to be 4.4%. We estimate the total multiplicative uncertainties to be 17.6% for $f_s \times \mathcal{B}(B_s^0 \to K_S^0\eta')$ and 23.4% for $\mathcal{B}(B_s^0 \to K_S^0\eta')$.

TABLE I. Summary of relative systematic uncertainties for $\mathcal{B}(B_s^0 \to \eta' K_S^0)$ and $f_s \times \mathcal{B}(B_s^0 \to \eta' K_S^0)$.

Source	Uncertainty (%)
$\sigma(\Upsilon(5S))$	4.7
$f_{B_s^{(*)0}\bar{B}_s^{(*)0}}$	1.87
$\mathcal{B}(\eta \to \gamma\gamma)$	0.2
$\mathcal{B}(\eta' \to \eta\pi^+\pi^-)$	0.7
$\mathcal{B}(K_S^0 \to \pi^+\pi^-)$	0.05
MC statistics	0.11
π reconstruction	1.4
η reconstruction	4.1
K_S^0 reconstruction	1.4
PDF parametrization	11.9
PID selection	2.4
Background suppression	4.4
Subtotal (without f_s)	17.6
f_s	15.4
Total	23.4

To estimate the upper limit using the frequentist approach [30], an 80% confidence-level (C.L.) belt (including systematic uncertainties) is prepared. To prepare this belt, we generate MC pseudoexperiments according to signal and background PDFs described previously. For each experiment, we generate 800 background events, which is, approximately, the number of background events obtained from fitting $\Upsilon(5S)$ data. We generate toy MC samples with the number of signal events in the range between 0 and 15. For each number of signal MC events we generate 2000 pseudoexperiments, obtain the number of signal events from a 3D fit and smear the resulting distributions of signal yields using the Gaussian σ of the total systematic uncertainty. The overall uncertainty is obtained by combining the uncertainty in the yield, σ, with the multiplicative uncertainty δ using the following formula [31]:

$$(N \pm \sigma)(1 \pm \delta) = N \pm (\sigma \oplus N\delta \oplus \sigma\delta), \qquad (3)$$

where $\oplus$ denotes addition in quadrature. We use the results of our pseudoexperiments to prepare an 80% classical confidence belt (without ordering), for which the lower and upper ends of respective confidence intervals correspond to the values for which 10% of fitting results lie below and above the boundary of the contour. We use this 80% confidence belt and its lower 10% sideband to estimate a 90% C.L. upper limit on the number of signal events in data to be 2.1, corresponding to a 90% C.L. upper limit on the branching fraction $\mathcal{B}(B_s^0 \to \eta' K_S^0) < 8.16 \times 10^{-6}$. We also estimate a 90% C.L. upper limit on the product $f_s \times \mathcal{B}(B_s^0 \to \eta' K_S^0) < 1.64 \times 10^{-6}$. The confidence intervals prepared using this statistical method are known to slightly "overcover" for the number of signal events [32], therefore resulting in a conservative upper limit.

In summary, we search for the charmless rare decay $B_s^0 \to \eta' K_S^0$ using the full data sample collected by the Belle experiment at $\Upsilon(5S)$ resonance. We find no statistically significant signal and set 90% C.L. upper limits $\mathcal{B}(B_s^0 \to \eta' K_S^0) < 8.16 \times 10^{-6}$ and $f_s \times \mathcal{B}(B_s^0 \to \eta' K_S^0) < 1.64 \times 10^{-6}$. Our results are the only experimental information currently available for this decay channel, and the reported 90% C.L. upper limit on the branching fraction is several times larger than the current theoretical predictions based on QCDF, SCET and flavor SU(3) symmetry [3–7]. This decay should be further searched for by the Belle II experiment [33] at the next-generation B-factory SuperKEKB, where its discovery would require $\Upsilon(5S)$ statistics of the order of 2 ab^{-1}.

We thank the KEKB group for the excellent operation of the accelerator; the KEK cryogenics group for the efficient operation of the solenoid; and the KEK computer group, and the Pacific Northwest National Laboratory (PNNL) Environmental Molecular Sciences Laboratory (EMSL) computing group for strong computing support; and the National Institute of Informatics, and Science Information NETwork 5 (SINET5) for valuable network support. We acknowledge support from the Ministry of Education, Culture, Sports, Science, and Technology (MEXT) of Japan, the Japan Society for the Promotion of Science (JSPS), and the Tau-Lepton Physics Research Center of Nagoya University; the Australian Research Council including grants No. DP180102629, No. DP170102389, No. DP170102204, No. DP150103061, No. FT130100303; Austrian Federal Ministry of Education, Science and Research (FWF) and FWF Austrian Science Fund No. P 31361-N36; the National Natural Science Foundation of China under Contracts No. 11435013, No. 11475187, No. 11521505, No. 11575017, No. 11675166, No. 11705209; Key Research Program of Frontier Sciences, Chinese Academy of Sciences (CAS), Grant No. QYZDJ-SSW-SLH011; the CAS Center for Excellence in Particle Physics (CCEPP); the Shanghai Science and Technology Committee (STCSM) under Grant No. 19ZR1403000; the Ministry of Education, Youth and Sports of the Czech Republic under Contract No. LTT17020; Horizon 2020 ERC Advanced Grant No. 884719 and ERC Starting Grant No. 947006 "InterLeptons" (European Union); the Carl Zeiss Foundation, the Deutsche Forschungsgemeinschaft, the Excellence Cluster Universe, and the VolkswagenStiftung; the Department of Atomic Energy (Project Identification No. RTI 4002) and the Department of Science and Technology of India; the Istituto Nazionale di Fisica Nucleare of Italy; National Research Foundation (NRF) of Korea Grants No. 2016R1D1A1B01010135, No. 2016R1D1A1B02012900, No. 2018R1A2B3003643, No. 2018R1A6A1A06024970, No. 2019K1A3A7A09033840, No. 2019R1I1A3A01058933, No. 2021R1A6A1A03043957, No. 2021R1F1A1060423, No. 2021R1F1A1064008; Radiation Science Research Institute, Foreign Large-size Research Facility Application Supporting project, the Global Science Experimental Data Hub Center of the Korea Institute of Science and Technology Information and KREONET/GLORIAD; the Polish Ministry of Science and Higher Education and the National Science Center; the Ministry of Science and Higher Education of the Russian Federation, Agreement 14.W03.31.0026, and the HSE University Basic Research Program, Moscow; University of Tabuk research grants No. S-1440-0321, No. S-0256-1438, and No. S-0280-1439 (Saudi Arabia); the Slovenian Research Agency Grant Nos. J1-9124 and P1-0135; Ikerbasque, Basque Foundation for Science, Spain; the Swiss National Science Foundation; the Ministry of Education and the Ministry of Science and Technology of Taiwan; and the United States Department of Energy and the National Science Foundation.

[1] A. J. Bevan, B. Golob, Th. Mannel, S. Prell, and B. D. Yabsley, Eur. Phys. J. C **74**, 3026 (2014); Report No. SLAC-PUB-15968; KEK Report No. 2014-3.
[2] E. Kou *et al.*, Prog. Theor. Exp. Phys. **2019**, 123C01 (2019).
[3] Y.-K. Hsiao, C.-F. Chang, and X.-G. He, Phys. Rev. D **93**, 114002 (2016).
[4] A. R. Williamson and J. Zupan, Phys. Rev. D **74**, 014003 (2006).
[5] A. Ali, G. Kramer, Y. Li, C.-D. Lü, Y.-L. Shen, W. Wang, and Y.-M. Wang, Phys. Rev. D **76**, 074018 (2007).
[6] H.-Y. Cheng and C.-K. Chua, Phys. Rev. D **80**, 114026 (2009).
[7] H.-Y. Cheng, C.-W. Chiang, and A.-L. Kuo, Phys. Rev. D **91**, 014011 (2015).
[8] T. E. Browder *et al.* (CLEO Collaboration), Phys. Rev. Lett. **81**, 1786 (1998).
[9] G. Bonvicini *et al.* (CLEO Collaboration), Phys. Rev. D **68**, 011101 (2003).
[10] An extensive list of theoretical literature on the subject of η' production in decays of heavy flavors could be found in D. S. Du, *International Workshop on Frontier of Theoretical Physics, P. R. China, 1999*, published in Proceedings (World Scientific, Singapore, 2001), pp. 49–51.
[11] S. Dubey *et al.* (Belle Collaboration), Phys. Rev. D **104**, 012007 (2021).

[12] A. L. Kagan and A. A. Petrov, arXiv:hep-ph/9707354.
[13] S. Kurokawa and E. Kikutani, Nucl. Instrum. Methods Phys. Res., Sect. A **499**, 1 (2003), and other papers included in this Volume; T. Abe *et al.*, Prog. Theor. Exp. Phys. **2013**, 03A001 (2013) and references therein.
[14] A. Abashian *et al.* (Belle Collaboration), Nucl. Instrum. Methods Phys. Res., Sect. A **479**, 117 (2002); also see Sec. II in J. Brodzicka *et al.*, Prog. Theor. Exp. Phys. **2012**, 4D001 (2012).
[15] S. Esen *et al.* (Belle Collaboration), Phys. Rev. D **87**, 031101(R) (2013).
[16] P. A. Zyla *et al.* (Particle Data Group), Prog. Theor. Exp. Phys. **2020**, 083C01 (2020).
[17] D. J. Lange, Nucl. Instrum. Methods Phys. Res., Sect. A **462**, 152 (2001).
[18] R. Brun *et al.*, GEANT Detector Description and Simulation Tool, CERN ebook 10.17181/CERN.MUHF.DMJ1 (1994).
[19] M. Feindt and U. Kerzel, Nucl. Instrum. Methods Phys. Res., Sect. A **559**, 190 (2006).
[20] H. Nakano, Search for new physics by a time-dependent CP violation analysis of the decay $B \to K_S \eta \gamma$ using the Belle detector, Ph.D. thesis, Tohoku University, 2014, Chap. 4 (unpublished).
[21] The Fox-Wolfram moments were introduced in G. C. Fox and S. Wolfram, Phys. Rev. Lett. **41**, 1581 (1978); The Fisher discriminant used by Belle, based on modified Fox-Wolfram moments (SFW), is described in K. Abe *et al.* (Belle Collaboration), Phys. Rev. Lett. **87**, 101801 (2001); K. Abe *et al.* (Belle Collaboration), Phys. Lett. B **511**, 151 (2001).
[22] R. A. Fisher, Ann. Eugenics **7**, 179 (1936).
[23] S. H. Lee *et al.* (Belle Collaboration), Phys. Rev. Lett. **91**, 261801 (2003).
[24] M. Oreglia, A study of the reactions $\psi' \to \gamma\gamma\psi$, Ph.D. thesis, 1980 [Report No. SLAC-0236]; T. Skwarnicki, A study of the radiative CASCADE transitions between the Upsilon-Prime and Upsilon resonances, Ph.D. thesis, 1986 [Report No. DESY-F31-86-02].
[25] H. Albrecht *et al.* (ARGUS Collaboration), Phys. Lett. B **241**, 278 (1990).
[26] J. Schumann *et al.* (Belle Collaboration), Phys. Rev. Lett. **97**, 061802 (2006).
[27] S. Ryu *et al.* (Belle Collaboration), Phys. Rev. D **89**, 072009 (2014).
[28] M. C. Chang *et al.* (Belle Collaboration), Phys. Rev. Lett. **98**, 131803 (2007).
[29] N. Dash *et al.* (Belle Collaboration), Phys. Rev. Lett. **119**, 171801 (2017).
[30] J. Neyman, Phil. Trans. R. Soc. A **236**, 333 (1937); Reprinted in *A Selection of Early Statistical Papers of J. Neyman*, (University of California Press, Berkely, 1967).
[31] P. Oskin *et al.* (Belle Collaboration), Phys. Rev. D **102**, 092011 (2020).
[32] G. J. Feldman and R. D. Cousins, Phys. Rev. D **57**, 3873 (1998).
[33] T. Abe *et al.* (Belle II Collaboration), arXiv:1011.0352; KEK Report No. 2010-1, 2010.